

## Modeling Large-Particle Deposition in Bends of Exhaust Ventilation Systems

Thomas M. Peters\* and David Leith

*Department of Environmental Sciences and Engineering, The University of North Carolina, Chapel Hill, North Carolina, USA*

---

**A new model is presented to describe particle deposition in 90° bends of exhaust ventilation systems. This model accounts for non-Stokes particle motion and for variable deposition patterns as a function of particle Stokes number. Estimates made with the new model and with two models previously published were compared to measurements of deposition in bends with geometries, particle characteristics, and airflow conditions similar to those found in industry—large duct diameters (15.4 and 20.3 cm), large particle sizes (19–140 μm), and turbulent airflow (Re = 203,000 and Re = 368,000). Whereas the two models published previously explain 30% or less of the variability in the data, the new model explains 85%. The mean residual with the new model, 0.6%, is nearer to zero than that of the two other models, 3.6% and 9.8%. The new model is applicable to mists and to solid particles that stick to bend walls.**

---

### INTRODUCTION

Ducts are prevalent in modern buildings; they supply conditioned air and exhaust contaminated air. When particles deposit in these ducts, problems can arise that range from sick building syndrome in office buildings (Muhic and Butala 2004) to fires in restaurant kitchens (Gerstler 2002). In factories, particles that deposit in exhaust ducts can restrict airflow, create fire hazards, cause failure of overhead supports, and present growth media for

biological contaminants (May and Berard 1987; Gregory et al. 1991).

Models are available to estimate particle deposition as a function of duct geometry, airflow conditions, and particle characteristics. Generally, the deposition of particles smaller than 20 μm from laminar airflow is well understood (Brockmann 2001). However, exhaust ducts commonly transport particles larger than 20 μm in highly turbulent airflow (100,000 < Reynolds number; Re < 1,000,000). Although Sippola and Nazaroff (2003) provide a model to estimate particle deposition in straight, rectangular ducts at high Re, models remain unavailable to estimate the deposition of large particles in bends under turbulent airflow conditions.

A bend in an exhaust system introduces several scales of curvilinear motion to duct flow. The largest of these motions occurs as the bend reorients the direction of the airflow: its radius is of the size of the centerline radius of curvature of the bend,  $R_b$ . As centrifugal force drives the central air core toward the outer wall, a smaller secondary flow develops that is of the size of the duct radius,  $a$  (Ito 1987), and its strength is characterized by the Dean number,  $De$  (Berger and Talbot 1983):  $De = Re/(R_0)^{1/2}$ , where  $R_0$  is the curvature ratio or the radius of the bend divided by the radius of the duct ( $R_0 = R_b/a$ ).

For moderately turbulent flow (Re < 10,000), Pui et al. (1987) used a well-mixed model to describe particle deposition in small-diameter bends. McFarland et al. (1997) empirically modeled numerical simulations of particle impaction in bends for Re up to 19,800. Peters and Leith (2004a) identified inadequacies in these models when applied to round bends in exhaust ventilation systems. Specifically, they showed that these models underrepresent drag force and overestimate deposition when particle motion is outside the Stokes regime. Further, they identified small but significant differences in particle deposition with changes in bend orientation.

The present work develops a new model to describe particle deposition in round, 90° bends for conditions typical of exhaust ventilation systems.

---

Received 19 January 2004; accepted 29 September 2004.

This work was made possible by a gift from Ford Motor Company and the United Auto Workers to support research in air engineering at the University of North Carolina at Chapel Hill, by a Department of Education Fellowship for Interdisciplinary Training in Environmental Engineering, and by a National Institute of Occupational Safety and Health Educational Resource Center Training Grant (T42/CCT410423-09).

\*New Address: Department of Occupational and Environmental Health The University of Iowa, Iowa City, IA 52242.

Address correspondence to David Leith, Department of Environmental Sciences and Engineering, The University of North Carolina, Chapel Hill, NC 27599, USA. E-mail: david.leith@unc.edu

**Table 1**  
Test conditions for 90° bends from Peters and Leith (2004a).

Test number	Test description	Re (De)	R <sub>0</sub>	Construction	Orientation
#1	Base	203,000 <sup>a</sup> (91,000)	5	Smooth	H-H
#2	Base + orientation	203,000 (91,000)	5	Smooth	<b>H-V</b>
#3	Base + construction	203,000 (91,000)	5	<b>Gored</b>	H-H
#4	High Re, small R <sub>0</sub>	<b>368,000<sup>b</sup> (212,000)</b>	<b>3</b>	Smooth	H-H
#5	High Re, large R <sub>0</sub>	<b>368,000 (106,000)</b>	<b>12</b>	Smooth	H-H

<sup>a</sup>U<sub>0</sub> = 20.0 m s<sup>-1</sup>; D<sub>duct</sub> = 0.152 m.

<sup>b</sup>U<sub>0</sub> = 27.1 m s<sup>-1</sup>; D<sub>duct</sub> = 0.203 m.

Bold, italic font identifies parameters that deviate from the base condition.

## METHODS

### Data Set

The data used here were taken from Peters and Leith (2004a) for tests in which the bend angle was 90° (Table 1). In Test #1, they identified a base condition as Re = 203,000, smooth internal walls (Figure 1a), R<sub>0</sub> = 5, and orientation such that air entered and exited the bend horizontally (H-H). In Test #2 they modified the base condition so that air entered the bend horizontally and exited vertically (H-V), and in Test #3 they modified it so that the construction of the bend was gored (Figure 1b). They conducted the remaining tests with Re = 368,000: in Test #4 the bend curved tightly (R<sub>0</sub> = 3) and in Test #5 the bend curved gradually (R<sub>0</sub> = 12). For these conditions, the De ranged from 91,000 to 212,000.

In each test, particle deposition by size was measured in triplicate with the methods presented by Peters and Leith (2004b); a brief overview of this method is provided here. Figure 2 illustrates the experimental setup. Upstream of the test bend,

an aerosol generator introduced polydisperse glass spheres that ranged in size from 5 to 150 μm. To capture and retain particles that hit the wall, the interior of the bend was coated with petroleum jelly. Circular sampling grids were cut from welded-wire mesh, coated with petroleum jelly, and alternately inserted into the duct upstream and downstream of the bend. Upstream velocity profiles were characteristic of fully developed pipe flow (Tennekes and Lumley 1972), and particle profiles were uniform in concentration and size distribution.

After sampling, the collected particles were recovered from the grids using a hexane extraction procedure and then sized using a sedimentation pipette (Silverman et al. 1971). Cumulative mass distributions were fitted with a log-normal distribution: all distributions were fit with r<sup>2</sup> > 0.8. From these distributions, deposition was calculated for each size interval (i) as

$$\eta_{\text{dep},i} = \left(1 - \frac{dM_{i,\text{down}}}{dM_{i,\text{up}}}\right), \quad [1]$$

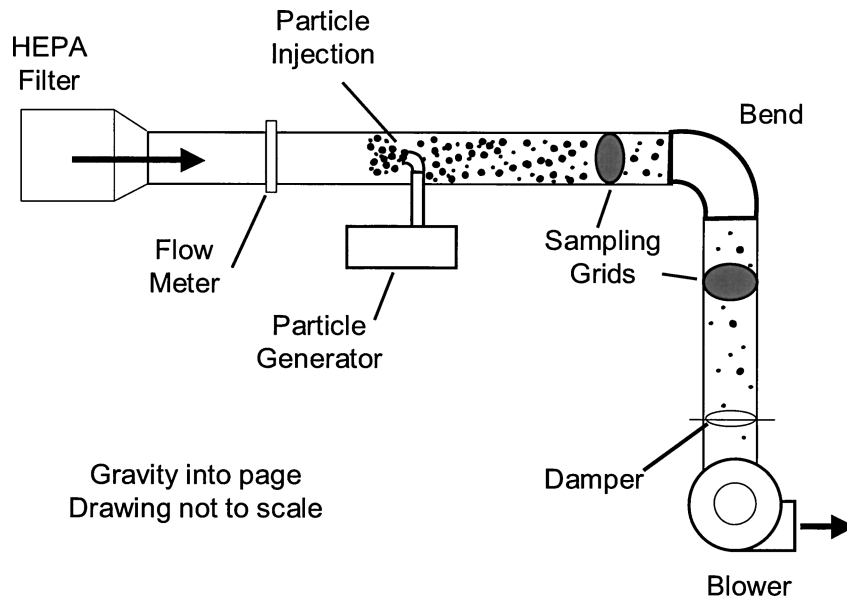


**Figure 1.** Schematic diagram of bends, (a) smooth and (b) gored.

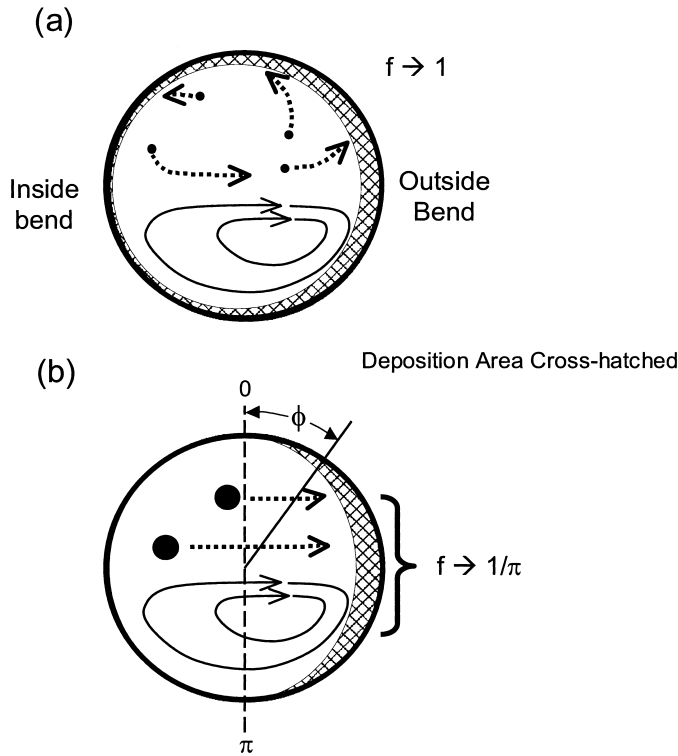


**Figure 2.** Experimental setup (a) smooth and (b) gored.

where  $dM_{i,down}$  is the downstream and  $dM_{i,up}$  is the upstream interval mass associated with the log-normal fit.

### Model Formulation

The new model considered particle deposition due to gravitational settling and inertial impaction. The fraction of particles that penetrate through a duct due to gravitational settling,  $P_{grav}$ , was estimated as:

$$P_{grav} = \exp\left(-\frac{4V_{ts}L}{\pi D_{duct}U_0}\right), \quad [2]$$

where  $V_{ts}$  is the terminal settling velocity of the particle,  $L$  is the length through which gravity contributes to deposition,  $D_{duct}$  is the duct diameter, and  $U_0$  is the airflow velocity entering the bend (Brockmann 2001). For the bend with the largest length, >90% of 100  $\mu\text{m}$  particles and >95% of 70  $\mu\text{m}$  particles penetrate through the bend. Thus, in comparison to inertial impaction, gravitational settling was relatively unimportant, and the effect of gravity was not included in the model.

For inertial impaction, the assumption of well-mixed conditions allows the fraction of particles that penetrates a bend ( $P$ ) to be expressed as

$$P = \exp\left(-\frac{A_e V_r}{Q}\right) = \exp\left(-\frac{A_e V_r}{\pi a^2 U_0}\right), \quad [3]$$

where  $V_r$  is the radial velocity of the particle,  $A_e$  is the effective deposition surface area, and  $Q$  is the airflow rate (Pui et al. 1987).

Assuming rotational flow and equating the centrifugal force with the Newtonian drag force,  $V_r$  was estimated using

$$V_r = \sqrt{\frac{4D_p \rho_p U_0^2}{3R_b \rho_f C_D}}, \quad [4]$$

where  $D_p$  is the particle diameter,  $\rho_p$  is the particle density,  $\rho_f$  is the fluid density, and  $C_D$  is the coefficient of drag.  $C_D$  is a function of particle Reynolds number ( $Re_p$ ), which is a function of  $V_r$ . According to Hinds (1999),  $V_r$  can be estimated by iterating Equation (4) and the following equation:

$$C_D = \frac{24}{Re_p} \left(1 + \frac{Re_p^{2/3}}{6}\right). \quad [5]$$

Secondary airflow in a bend causes the effective deposition area term,  $A_e$ , in Equation 3 to be a fraction of the total internal surface area of the bend,  $f$ :

$$A_e = f(2\pi aL) = f(2\pi aR_b\theta), \quad [6]$$

where  $L$  is the axial length of the bend and  $\theta$  is the angle in radians through which the bend sweeps. With substitutions, Equation (3) becomes

$$P = \exp\left(-2f \frac{V_r R_b \theta}{aU_0}\right). \quad [7]$$

In exhaust ducts, particle motion is often outside the Stokes regime; thus, a transition Stokes number ( $Stk_T$ ) was formulated as

$$Stk_T = \frac{\text{distance traveled by particle}}{\text{distance required to hit wall}} = \frac{V_r t}{a} = \frac{V_r R_b \theta}{aU_0}, \quad [8]$$

where  $t$  is the time for the air to pass through the bend and penetration is

$$P = \exp(-2f Stk_T). \quad [9]$$

Whereas  $Stk_T$  is easily estimated from experimental conditions, the factor  $f$  requires more consideration.

As depicted in Figure 3, the value of  $f$  depends on particle Stokes number. For small Stokes numbers, particles are easily entrained by the secondary flow and particle deposits occur over a relatively large surface area (Figure 3a). Thus,

$$\lim_{Stk_T \rightarrow 0} (f) = 1. \quad [10]$$

For large Stokes numbers, particles are relatively unaffected by the secondary flow, and the vector of outward radial velocity is directed solely towards the outside wall (Figure 3b). Here,  $f$  is the integrated component of radial velocity normal to the outside

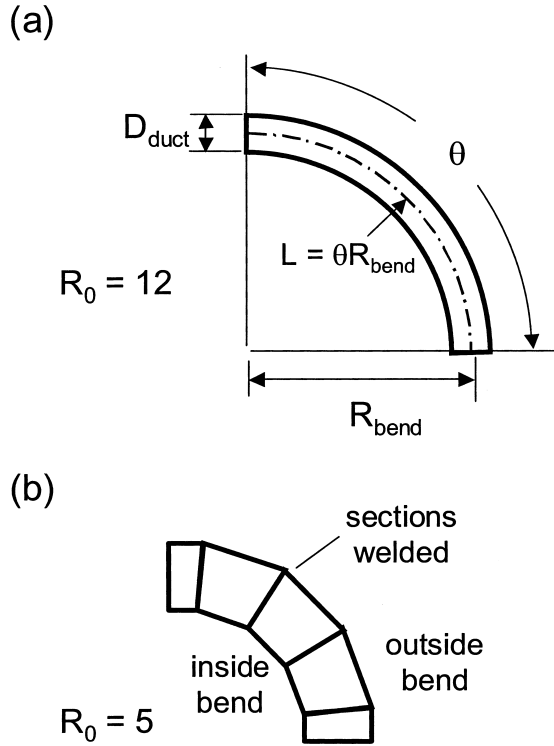


**Figure 3.** Duct cross section showing the secondary flow (lower half of duct) and particles entrained in this flow (upper half of duct) for (a) small  $Stk_T$  and (b) large  $Stk_T$ .

wall,  $V_r \sin(\phi)$ , divided by  $V_r$  and the duct circumference in radians:

$$f = \frac{V_r \int_0^\pi \sin(\phi) d\phi}{V_r 2\pi} = \frac{-\cos(\phi)|_0^\pi}{2\pi} = \frac{1}{\pi}. \quad [11]$$

Thus,

$$\lim_{Stk_T \rightarrow \infty} (f) = \frac{1}{\pi}. \quad [12]$$

A semiempirical relationship was developed to describe  $f$  between these limits. Equation (9) was rearranged as

$$f = -\frac{\ln(P_x)}{2Stk_T}, \quad [13]$$

where  $P_x$  is fractional penetration from the data set. As shown in Figure 4,  $f$  values approached the limits discussed above for small and large  $Stk_T$ . These data were fit with the following three-parameter model:

$$f = \frac{1}{\pi} + \left(1 - \frac{1}{\pi}\right) \exp\left(-\frac{Stk_T}{1.218}\right). \quad [14]$$

Two of the three parameters in Equation (14) came from the limits for  $f$ , the first term from Equation (12) and the coefficient

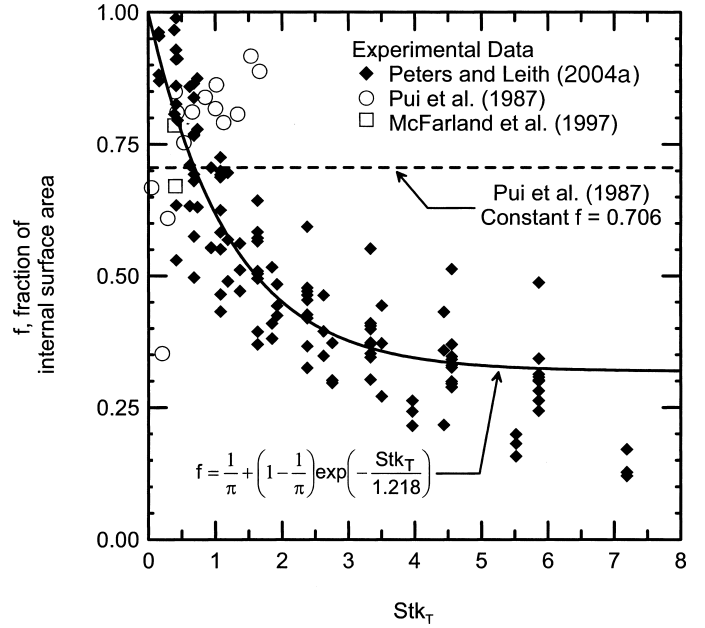


**Figure 4.** Fraction of total internal surface area where particles deposit ( $f$ ) versus  $Stk_T$ .

of the second term from Equation (10). The factor of 1.218 came from a least-squares fit between Equation (14) and the data.

To use the new model to determine deposition in a duct bend for a particle of given size; (1) iteratively calculate  $V_r$  with Equation (4) and Equation (5), (2) calculate  $Stk_T$  with Equation (8), (3) calculate  $f$  with Equation (14), (4) calculate  $P$  with Equation (9), and (5) calculate the percentage of particles that deposits in the bend,  $\eta_{dep}$ , as

$$\eta_{dep} = (1 - P) * 100\%. \quad [15]$$

In this work, all calculations were carried out in a spreadsheet (Excel, Microsoft, Redmond, WA, USA). A macro within the spreadsheet was written to estimate  $V_r$  by iterating Equations (4) and (5). For example, a  $30 \mu\text{m}$  spherical glass particle ( $\rho_p = 2450 \text{ kg m}^{-3}$ , aerodynamic diameter =  $50 \mu\text{m}$ ) in Test #1 yielded the following values for each step above: (1)  $V_r = 4.5 \text{ m s}^{-1}$ , (2)  $Stk_T = 1.76$ , (3)  $f = 0.48$ , (4)  $P = 0.185$ , and (5)  $\eta_{dep} = 81.5\%$ .

### Model Comparisons

Estimates made with the new model were compared with three other models. The first of these, published by McFarland et al. (1997), expresses fractional penetration as

$$P = \exp\left(\frac{4.61 + a_m \theta Stk}{1 + b_m \theta Stk + c_m \theta^2 Stk^2 + d_m \theta^2 Stk}\right) \times \frac{1}{100\%}, \quad [16]$$

where  $a_m$ ,  $b_m$ ,  $c_m$ , and  $d_m$  are coefficients found using a curve-fitting program, and  $Stk$  is the particle Stokes number assuming laminar conditions ( $Stk = \tau U_0/a$ ). An error appears in the

published coefficient for the second term in the numerator of coefficient  $d_m$ . Equation (13) of McFarland et al. (1997) should read

$$\begin{aligned} a_m &= -0.9526 - 0.05686R_0, \\ b_m &= \frac{-0.297 - 0.0174R_0}{1 - 0.07R_0 + 0.0171R_0^2}, \\ c_m &= -0.306 + \frac{1.895}{\sqrt{R_0}} - \frac{2.0}{R_0}, \\ d_m &= \frac{0.131 - 0.0132R_0 + 0.000383R_0^2}{1 - 0.129R_0 + 0.0136R_0^2}. \end{aligned} \quad [17]$$

The second model, originally published by Pui et al. (1987) and later modified to include bend angle by Brockmann (1993), is

$$P = \exp[-(2)(0.706) \text{Stk } \theta], \quad [18]$$

where the constant, 0.706, was determined by Pui et al. (1987) as the average  $f$  value from their experiments. For the third comparison, the model of Pui et al. (1987) was corrected for particle motion outside the Stokes regime by substituting  $\text{Stk}_T$  for  $\text{Stk } \theta$  in Equation (18). In all comparisons, percentage depositions were calculated from fractional penetrations using Equation (15).

For each model, the method of least squares was used to calculate the square of the correlation coefficient,  $r^2$ , and the  $F$  statistic. The mean residual and the standard deviation of the residual were also calculated. The experimental variability associated with the smallest particle diameter in the experiments obscured model evaluation; thus, statistical analyses were limited to data where particle diameter was between 19 and 140  $\mu\text{m}$ .

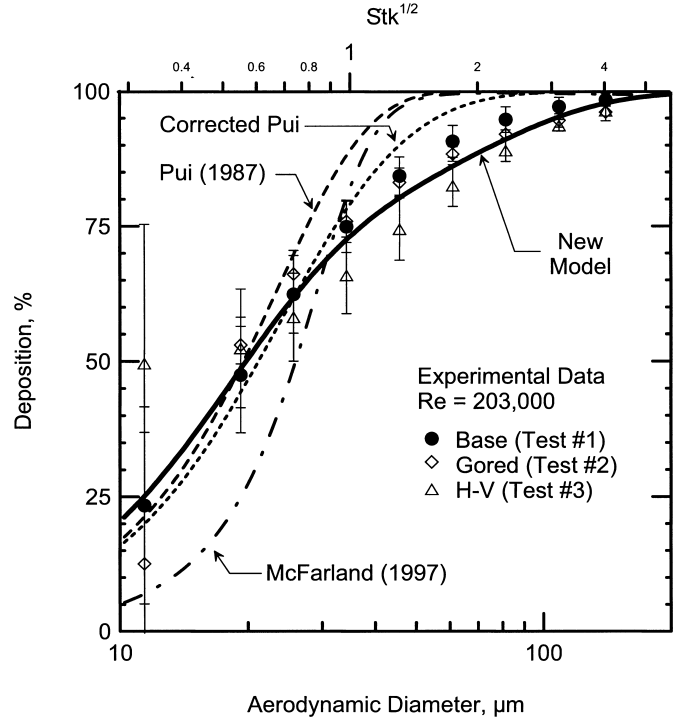
**RESULTS**

Table 2 presents results for each model. The  $r^2$  value ranged from 0.04 for the model of McFarland et al. (1997) to 0.85 for the new model. The  $F$  value was much larger for the new model,  $F = 699$ , than for the McFarland et al. (1997) model,  $F = 5$ , the Pui et al. (1987) model,  $F = 48$ , or for the corrected Pui model,  $F = 190$ . Mean residual, an indicator of systematic bias, was greatest for the Pui et al. (1987) model, 9.8%, and least for the new model, 0.6%. Standard deviations of the residuals were

**Table 2**  
Fit results for each model<sup>a</sup>

Model name	$r^2$	F (p value)	Mean residual, %	Std. dev. residual, %
McFarland et al. (1997)	0.04	5 (0.02)	3.6	14.5
Pui et al. (1987)	0.29	48 (<0.001)	9.8	8.3
Corrected Pui	0.62	190 (<0.001)	5.1	7.9
New model	0.85	699 (<0.001)	0.6	5.8

<sup>a</sup>Number of data points analyzed,  $n = 120$ .



**Figure 5.** Deposition versus particle size estimated with models and measured experimentally for tests where  $Re = 203,000$ .

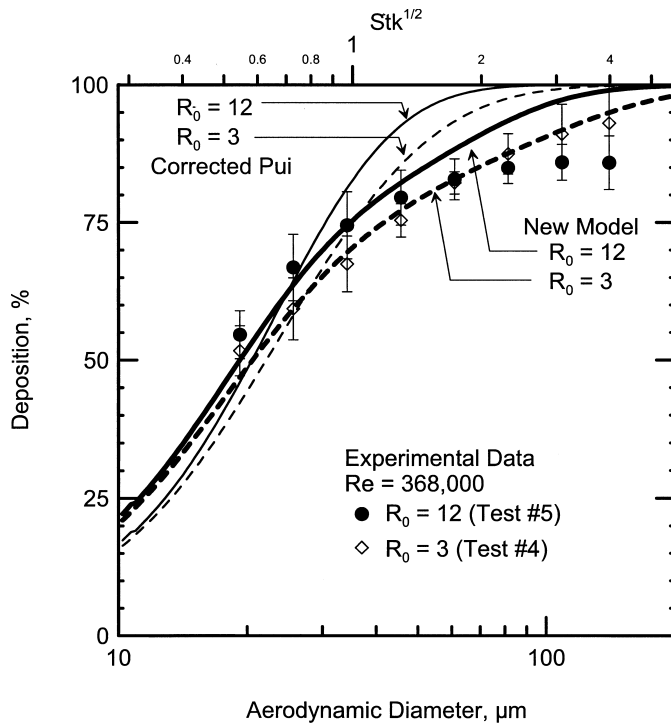
greatest for the McFarland et al. (1997) model, 14.5%, and least for the new model, 5.8%.

Figure 5 compares model estimates for deposition by particle size to the data for tests where  $Re = 203,000$  (Test #1, Test #2, and Test #3). For particles smaller than 30  $\mu\text{m}$ , the Pui et al. (1987) model estimates agreed well with the data, but the McFarland et al. (1997) model estimates were lower than the data. For larger particles, both earlier models overestimated deposition. Estimates made with the new model agreed relatively well with the data for all particle sizes.

Figure 6 compares new model estimates and corrected Pui model estimates to the data for tests where  $Re = 368,000$  (Test #4 and Test #5). For particles smaller than 30  $\mu\text{m}$ , estimates made with the new model and the corrected Pui model were similar and generally agreed with the data. For larger particles, the corrected Pui model overestimated deposition. The new model estimates agreed with the data somewhat better. For both models and for all particle sizes, deposition estimates were greater for the gradual bend ( $R_0 = 12$ ) than for the tight bend ( $R_0 = 3$ ).

**DISCUSSION**

Estimates of particle deposition made with the two earlier models did not agree particularly well with experimental data from exhaust bends, especially for particles larger than about 30  $\mu\text{m}$  in diameter. These models were developed using data from experiments where particle motion was within, or nearly within, the Stokes regime,  $Re_p < 3$ . Thus, they underestimated drag forces and overestimated deposition for larger particles in



**Figure 6.** Deposition versus particle size estimated with models and measured experimentally for tests where  $Re = 368,000$ .

exhaust bends, where  $Re_p$  ranged up to 200. Consequently, as shown in Table 2, these models fit the data used here with relatively low  $r^2$ , low  $F$ , high mean residual, and high standard deviation of the residual.

The corrected Pui model, which takes into account particle motion outside the Stokes region, explained more than twice the variability in the experimental data than did the original Pui et al. (1987) model. This observation illustrates the importance of correcting the drag force when particle motion is outside of the Stokes regime. However, the corrected Pui model still overestimated deposition for particles larger than about  $30 \mu\text{m}$ .

Estimates of particle deposition made with the new model agreed well with the experimental data for all particle sizes. Whereas the new model uses the semiempirical relationship for  $f$  given in Equation (14), the Pui et al. (1987) model and the corrected Pui model use a constant value for  $f$  of 0.706. Thus, where  $f$  calculated with Equation (14) was less than 0.706 (i.e.,  $Stk_T$  greater than 0.7), new model estimates were lower than the corrected Pui model estimates and agreed better with the data. Because the data used to develop the new model and the data used to compare the models were the same, the relatively good fit with the new model was not unexpected.

For  $Stk_T > 2$ , some values of  $f$  calculated from the data deviated from those estimated from Equation (14), e.g., see Figure 4. In Test #1, experimental  $f$  values were consistently greater than Equation (14) estimates. However, in Test #5 for  $Stk_T > 3$ , the experimental  $f$  values were consistently lower than the estimates, and lower than the theoretical limit identified in Equation (12).

The longer time required to pass through the gradual bend of Test #5 might have allowed gravity settling to alter deposition patterns in a manner slightly different from those in the other tests.

As shown in Figure 4 for  $Stk_T < 2$ ,  $f$  values computed from exhaust bends are generally consistent with those from Pui et al. (1987) and McFarland et al. (1997). However,  $f$  values from Pui et al. (1987) exhibited a trend opposite that of the data used here. Perhaps particle behavior in a large-diameter bend with highly turbulent airflow is different from that in the small-diameter bends with moderately turbulent airflow studied by Pui et al. (1987).

Consistent with the data in Figure 6 for particles between 30 and  $60 \mu\text{m}$ , new model estimates of particle deposition were slightly greater for the gradual bend (Test #5,  $R_0 = 12$ ) than for the tight bend (Test #4,  $R_0 = 3$ ). As the duct radius was the same for both tests, the bend radius,  $R_b$ , was larger for the bend with the larger  $R_0$ . Outward radial velocity is inversely proportional to  $R_b^{1/2}$  (Equation (4)), but the time for the air to pass through the bend is directly proportional to  $R_b$  (Equation (7)). Thus,  $Stk_T$  is proportional to  $R_b^{1/2}$ , and model estimates are greater when the bend curves more gradually.

Although the new model offers improvement over other models, it does not explain some features in the data. For particles larger than  $60 \mu\text{m}$ , Figure 6 shows that new model estimates were less for the tight bend than for the gradual bend, but the data show an opposite trend. Further, as gravity was assumed to be negligible, the new model does not account for the differences in particle deposition between orientations shown in Figure 5 (H-H versus H-V).

The experimental data modeled in this work was limited to  $91,000 < De < 212,000$ . Over this range, the fraction of the internal area surface area where particles deposit ( $f$ ) did not show a dependence on  $De$ . However, the factor  $f$  should increase with increasing  $De$  because stronger secondary flow will encourage particles to deposit over a larger surface area. Future work should investigate this trend further.

## CONCLUSION

This work presents a new model to estimate particle deposition in round,  $90^\circ$  duct bends with highly turbulent airflows. The new model accounts for particle motion outside the Stokes regime and for variable deposition patterns as a function of particle Stokes number. The model is applicable to deposition of droplets or solid particles where duct walls are sticky.

## NOMENCLATURE

$a$	duct radius
$A_e$	effective deposition area
$a_m, b_m, c_m, d_m$	constants used in McFarland et al. (1997)
$C_c$	Cunningham slip correction factor
$C_D$	coefficient of drag
$D_{\text{duct}}$	duct diameter
$De$	Dean number = $\frac{Re}{\sqrt{R_0}} = \frac{\sqrt{\rho_f^2 U_0^2}}{\mu_f R_b}$

$D_p$	particle diameter
f	fraction of internal surface area acting to deposit particles
H-H	horizontal-to-horizontal orientation
H-V	horizontal-to-vertical orientation
L	arc length through which bend sweeps
P	fractional penetration
$P_x$	fractional penetration determined experimentally
Q	airflow rate
$R_0$	curvature ratio = $\frac{R_b}{a}$
$R_b$	the centerline radius of curvature of the bend
Re	flow Reynolds number = $\frac{D_{duct}U_0}{\nu}$
$Re_p$	Reynolds number = $\frac{D_p V}{\nu}$
$U_0$	mean axial velocity upstream of the bend
V	relative velocity between the particle and the surrounding air
$V_r$	particle radial velocity
$V_{ts}$	particle terminal settling velocity
Stk	particle Stokes number based on duct radius = $\frac{\tau U_0}{a}$
Stk <sub>T</sub>	transition Stokes number = $\frac{V_r R_b \theta}{a U_0}$
t	time for air to pass through a bend
$\eta$	percent of incoming particles that deposit
$\mu_f$	fluid dynamic viscosity
$\nu$	fluid kinematic viscosity
$\theta$	angle through which the bend sweeps
$\phi$	angle
$\rho_f$	fluid density
$\rho_p$	particle density
$\tau$	particle relaxation time = $\frac{C_c \rho_p D_p^2}{18 \mu_f}$

### Subscripts

dep	estimated with the model
x	experimental

mean	mean value
grav	gravity

### REFERENCES

- Berger, S. A., and Talbot, L. (1983). Flow in Curved Pipes, *Ann. Rev. Fluid Mech.* 15:461–512.
- Brockmann, J. E. (1993). Sampling and Transport of Aerosol. In *Aerosol Measurement: Principles, Techniques, and Applications*, edited by K. Willeke and P. A. Baron. Van Nostrand Reinhold, New York, pp.77–111.
- Brockmann, J. E. (2001). Sampling and Transport of Aerosol. In *Aerosol Measurement: Principles, Techniques, and Applications*, edited by P. A. Baron and K. Willeke. Van Nostrand Reinhold, New York, pp. 143–195.
- Gerstler, W. D. (2002). New Rules for Kitchen Exhaust. *ASHRAE J.* Nov.:26–33.
- Gregory, W. S., Martin, R. A., White, B. W., Nichols, B. D., Smith, P. R., Leslie, I. H., Fenton, D. L., Gunaji, M. V., and Blythe, J. R. (1991). Fires in Large Scale Ventilation Systems. *Nuclear Engineering and Design* 125(3):337–345.
- Hinds, W. C. (1999). *Aerosol Technology: Properties, Behavior, and Measurement of Airborne Particles*. John Wiley & Sons, Inc., New York, pp. 242–248.
- Ito, H. (1987). Flow in Curved Pipes, *JSME Int. J.* 30:543–552.
- May, D. C., and Berard, D. L. (1987). Fires and Explosions Associated with Aluminum Dust from Finishing Operations, *J. Hazardous Mater.* 17(1):81–88.
- McFarland, A. R., Gong, H., Muyschondt, A., Wente, W. B., and Anand, N. K. (1997). Aerosol Deposition in Bends with Turbulent Flow, *Environ. Sci. Technol.* 31:3371–3377.
- Muhic, S., and Butala V. (2004). The Influence of Indoor Environment in Office Buildings on Their Occupants: Expected-unexpected. *Building Environ.* 39(3):289–296.
- Peters, T. M., and Leith, D. (2004a). Particle Deposition in Industrial Duct Bends, *Ann. Occup. Hygiene* 48(5):483–490.
- Peters, T. M., and Leith, D. (2004b). Measurement of Particle Deposition in Industrial Ducts, *Journal of Aerosol Science* 34(5):529–540.
- Pui, D. Y. H., Romay-Novas, F., and Liu, B. Y. H. (1987). Experimental Study of Particle Deposition in Bends of Circular Cross Section, *Aerosol Sci. Technol.* 7:301–315.
- Silverman, L., Billings, C. E. et al. (1971). *Particle Size Analysis in Industrial Hygiene*. Academic Press, New York.
- Sippola, M. R., and Nazaroff, W. W. (2003). Modeling Particle Loss in Ventilation Ducts, *Atmos. Environ.* 37(39–40): 5597–5609.
- Tennekes, H., and Lumley, J. L. (1972). *A First Course in Turbulence*. The MIT Press, Cambridge, MA.